Journal of Alloys and Compounds 580 (2013) 125–130

Contents lists available at SciVerse ScienceDirect

Journal of Alloys and Compounds

journal homepage: www.elsevier.com/locate/jalcom

Cryomilling effect on the mechanical alloying behaviour of ferritic oxide dispersion strengthened powder with Y_2O_3

Jeoung Han Kim [a,*], Jae Hoon Lee [b], Jeon Yeong Min [a], Seong Woong Kim [a], Chan Hee Park [a], Jong Taek Yeom [a], Thak Sang Byun [c]

[a] Special Alloys Group, Korea Institute of Materials Science, Changwon, South Korea
[b] POSCO Technical Research Laboratories, Gwangyang-si, Jeonnam 545-090, South Korea
[c] Materials Science and Technology Division, Oak Ridge National Laboratory, Oak Ridge, TN 37831, USA

ARTICLE INFO

Article history:
Received 28 February 2013
Received in revised form 23 April 2013
Accepted 23 April 2013
Available online 2 May 2013

Keywords:
Oxide dispersion strengthened alloy
Mechanical alloying
Grain refinement
Nuclear reactor materials
X-ray diffraction

ABSTRACT

Cryogenic cooling effect on mechanical alloying of the mixture of Fe–14Cr–3W–0.1Ti and Y_2O_3 powders was investigated. The powder mixtures were ball milled for 40 h at room-temperature and −150 °C. Cryomilling produced much finer particle/grain size than conventional room-temperature milling. XRD diffraction peak intensity was much lower under cryomilling conditions due to formation of nano-size grains and increased residual microstrain. Absorption amounts of interstitial elements were considerably higher under cryomilling conditions.

1. Introduction

The advanced oxide-dispersion-strengthened (ODS) steels have great advantages in creep and irradiation resistance for high temperature reactor applications [1–4]. Recent progress shows that ultra-fine grained microstructures, with a high density of nanoclusters, can be produced by controlled ball milling and a consolidation process. During a high energy mechanical alloying (MA) process, deformation-induced dissolution or dissociation of Y_2O_3 powder into the matrix occurs [5,6], which can be explained by dislocation assisted mass transfer of the interstitial element from the oxides into the matrix [7]. Since the amount of defects or strains generated by MA plays a major role in oxide particle dissolution or dissociation, proper control of MA parameters not only will finely distribute the Y_2O_3 powder but can also improve other microstructural properties [8]. Thus, MA can be thought to be the most important step in ODS steels fabrication.

MA is a long-term continuous operation producing a lot of heat from friction, vibration and plastic deformation. If the heat cannot be discharged in time, it will directly affect the efficiency of milling and quality of the resulting powder. Although the MA behaviour is believed to be closely related to milling temperature, exact information on the cooling effect on MA of ODS is not yet available. Especially, cryomilling [9] in which the milling operation is carried out at cryogenic (very low) temperatures is expected to produce a few nano-sized particles that effectively strengthen ODS steel [10]. During MA, the formation of expected or unexpected alloy phases can be affected by the temperature of the powder and milling media because diffusion processes are involved. For example, the degree of solid solubility and the formation of amorphous or nanocrystalline phases may be different, depending on the milling temperature.

The present work was performed to clarify the cryomilling effect on powder ball milling of Fe-alloy + Y_2O_3, and to design a new manufacturing process for advanced ODS steel. To facilitate the experiments, we intentionally put highly excessive amounts of Y_2O_3 (15 wt.%) into Fe–14Cr–3W–0.1Ti pre-alloyed metal powder, instead of the 0.3 wt.% Y_2O_3 which is normal for this process. The larger amounts of Y_2O_3 permit the easy study of MA behaviour by XRD (X-ray diffractometer).

2. Experimental procedure

A pre-alloyed metal powder with chemical composition Fe–14Cr–3W–0.1Ti (wt.%) was mixed with the Y_2O_3 powder of 30–50 nm particle size, and then put into a milling chamber. MA was performed using a planetary milling machine in a high-purity Ar (99.999 wt.%) atmosphere for 1, 3, 5, 10, and 40 h at room-temperature and at −150 ± 10 °C. To lower the test temperature to −150 °C, a liquid nitrogen–air mixture was dripped onto the milling chamber, which had been carefully sealed with a ring specially designed for low temperature applications. After finishing the milling, the Ar pressure level was checked to ensure that the seal was intact.

* Corresponding author. Tel.: +82 55 280 3372.
E-mail addresses: kjh1754@kims.re.kr, kimjh000@gmail.com (J.H. Kim).

0925-8388/$ - see front matter © 2013 Elsevier B.V. All rights reserved.
http://dx.doi.org/10.1016/j.jallcom.2013.04.165

All the powder handling and sampling were performed in an argon-filled glove box. Chromium steel balls with diameters of 8 mm and 20 mm were used together for milling with a ball-to-powder weigh ratio of 20:1. The compositions of interstitial elements were measured using an inductively coupled plasma spectrometer before and after MA.

In order to investigate the powder morphology and Y_2O_3 particle distribution, a JSM-7001F and a JEM-2100F were used for SEM (scanning electron microscopy) and TEM (transmission electron microscopy), respectively. EBSD (electron backscattering diffraction) maps were taken on an EDAX-TSL system. Also, the structural evolution during MA was examined by using Rigaku-2500 XRD machine with a Cu Kα radiation. The variation of mean grain size and residual strain of the powders were estimated using the Williamson–Hall equation:

$$\beta \cdot \cos\theta = K\lambda/d + 4\varepsilon \cdot \sin\theta \quad (1)$$

where λ is the X-ray wavelength, β the full width at half maximum (FWHM), ε the residual microstrain, K the shape factor taken as 0.9, and d the mean grain size. By plotting $\beta\cdot\cos\theta$ against $4\sin\theta$, a straight line with gradient ε and intercept $K\lambda/d$ can be obtained. The β values from five planes (*i.e.* (211), (222), (400), (440), and (622)) of the Y_2O_3 were used in the calculation. Prior to the above analysis, the effect of instrumental broadening measured on large grained Y_2O_3 was subtracted from the experimental broadening using the Gausian–Gausian relationship [11]:

$$\beta_{exp}^2 = \beta^2 + \beta_{inst}^2 \quad (2)$$

where β_{exp} and β_{inst} are the FWHM of the experimental and instrumental profiles, respectively.

3. Results and discussion

3.1. Microstructural evolution

Fig. 1 shows the variation of powder morphology and size variation with milling time. The initial alloy powder had a spherical shape with diameter of 10–60 μm. A large number of Y_2O_3 particles that looked like cotton balls were noticed in the alloy powder. The particle size of the powders milled at room-temperature gradually increased with milling time and didn't reach steady-state for up to 10 h. Between the milling times of 10 and 40 h, agglomerated particles of particle size 40–100 μm were noticed. This means that the rate of welding, which tends to increase the average particle size, overwhelms the rate of fracturing for at least up to 10 h. In contrast, the cryomilled powders showed continuously decreasing size until they reached the final powder size of ~5 μm. Average particle size decreased rapidly during the first hours of milling, and then slowly decreased. Although average particle size was not much different, uniformity was much better in the powder milled for 40 h, than that milled for 10 h. Therefore, it can be concluded that particle refinement efficiency is much higher at −150 °C than at room-temperature.

Fig. 2 shows the EBSD photos for the ferrite phase in both powders after 40 h of milling. Cryomilled powder showed very fine equiaxed grains of ~280 nm; with nearly random texture orientation. In contrast, room-temperature milled powder revealed rather coarse, elongated grains (length ~800 nm). Also, aggregates of grains that had similar inverse pole figure indices were found. The KAM (Kernel average mis-orientation) analysis representing the mean angle between the crystallographic orientation of each pixel and those of its eight nearest neighbours [12] was calculated from the EBSD results. The KAM analysis in Fig. 2c and d provides interesting qualitative images of the dislocation or defect density [13] at the same areas shown in Fig. 2a and b. Cryomilled powders exhibited high KAM values at certain local areas, especially inside of small grains (less than ~400 nm) whereas room-temperature milled powders showed relatively moderate KAM distribution throughout the microstructure. This quantification indicates that local inhomogeneity increases faster under cryomilling conditions, which results in internal subgrain structure and consequently, a very fine grain structure.

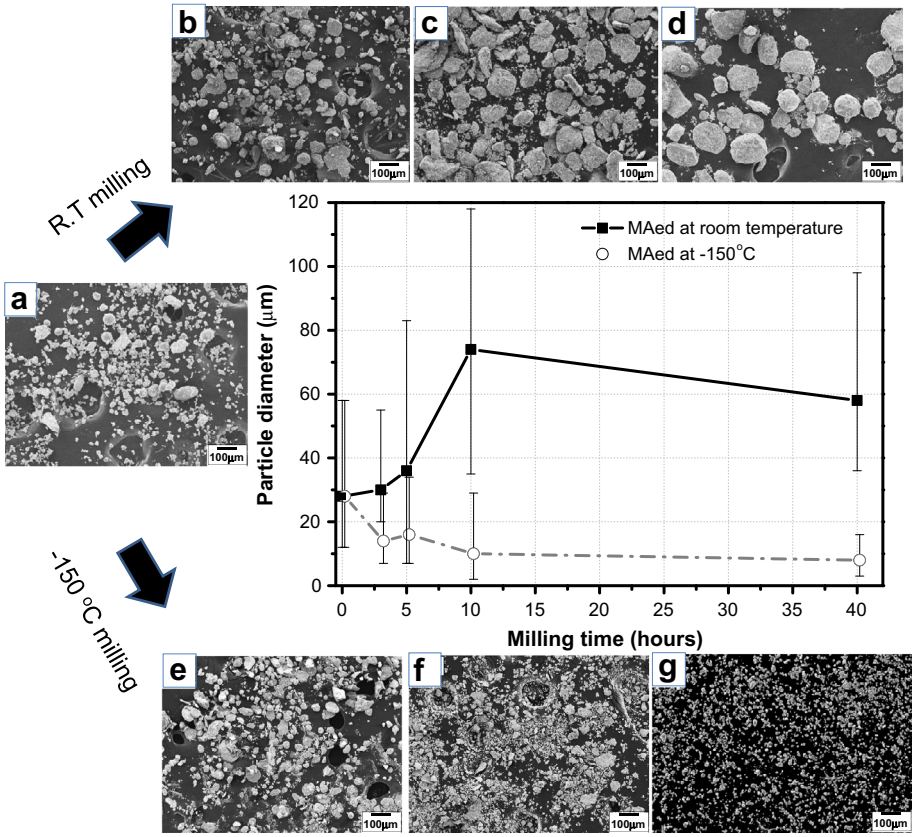

Fig. 1. The variation of powder particle size during MA: (a) initial powders and milled powders taken after MA for (b, e) 3 h, (c, f) 10 h and (d, g) 40 h, respectively.